J. Cell. Mol. Med. Vol 12, No 5B, 2008 pp. 2003-2014

Phage display selection of peptides that home to atherosclerotic plaques: IL-4 receptor as a candidate target in atherosclerosis

Hai-yan Hong [a], Hwa Young Lee [b], Wonjung Kwak [b], Jeongsoo Yoo [b], Moon-Hee Na [a], In Seop So [a], Tae-Hwan Kwon [a], Heon-Sik Park [c], Seung Huh [d], Goo Taeg Oh [e], Ick-Chan Kwon [f], In-San Kim [a, *], Byung-Heon Lee [a, *]

[a] Department of Biochemistry and Cell Biology, Cell & Matrix Research Institute, School of Medicine, Kyungpook National University, Daegu, Korea
[b] Department of Molecular and Nuclear Medicine, School of Medicine, Kyungpook National University, Daegu, Korea
[c] Department of Internal Medicine, School of Medicine, Kyungpook National University, Daegu, Korea
[d] Department of Surgery, School of Medicine, Kyungpook National University, Daegu, Korea,
[e] Division of Life and Pharmaceutical Sciences, Ewha Womens University, Seoul, Korea
[f] Korea Institute of Science and Technology, Seoul, Korea

Received: July 6, 2007; Accepted: November 23, 2007

Abstract

Imaging or drug delivery tools for atherosclerosis based on the plaque biology are still insufficient. Here, we attempted to identify peptides that selectively home to atherosclerotic plaques using phage display. A phage library containing random peptides was *ex vivo* screened for binding to human atheroma tissues. After three to four rounds of selection, the DNA inserts of phage clones were sequenced. A peptide sequence, CRKRLDRNC, was the most frequently occurring one. Intravenously injected phage displaying the CRKRLDRNC peptide was observed to home to atherosclerotic aortic tissues of low-density lipoprotein receptor-deficient ($Ldlr^{-/-}$) mice at higher levels than to normal aortic tissues of wild-type mice. Moreover, a fluorescein- or radioisotope-conjugated synthetic CRKRLDRNC peptide, but not a control peptide, homed *in vivo* to atherosclerotic plaques in $Ldlr^{-/-}$ mice, while homing of the peptide to other organs such as brain was minimal. The homing peptide co-localized with endothelial cells, macrophages and smooth muscle cells at mouse and human atherosclerotic plaques. Homology search revealed that the CRKRLDRNC peptide shares a motif of interleukin-4 receptor (IL-4) that is critical for binding to its receptor. The peptide indeed co-localized with IL-4 receptor (IL-4R) at atherosclerotic plaques. Moreover, the peptide bound to cultured cells expressing IL-4R on the cell surface and the binding was inhibited by the knockdown of IL-4R. These results show that the CRKRLDRNC peptide homes to atherosclerotic plaques through binding to IL-4R as its target and may be a useful tool for selective drug delivery and molecular imaging of atherosclerosis.

Keywords: atherosclerotic plaque • IL-4 receptor • LDL receptor • phage display • homing peptide

Introduction

Cardiovascular diseases are the leading cause of death in the developed countries. Atherosclerosis is the major contributor to the pathogenesis of acute myocardial and cerebral thrombosis [1]. Atherosclerosis is a chronic, progressive inflammatory disease, which develops in response to endothelial injury. Initiation of the injury is brought by pro-inflammatory cytokines and risk factors, such as hypercholesterolemia, smoking, hypertension and diabetes [2]. Atherosclerotic arteries have morphologically raised lesions referred to as atherosclerotic plaques. They are characterized by the deposition of lipids, inflammatory cells like macrophages and T lymphocytes, vascular smooth muscle cells and connective tissue within the arterial wall [1]. As the lesion

*Correspondence to: Byung-Heon LEE, In-San KIM,
Department of Biochemistry and Cell Biology, School of Medicine,
Kyungpook National University, 101 Dongin-Dong,
Jung-Gu, Daegu 700-421, Korea.
Tel.: +82-53-420-48 24(B-H.L.), +82-53-420-48 21(I-S.K.)
Fax: +82-53-422-1466
E-mail: leebh@knu.ac.kr(B-H.L.); iskim@knu.ac.kr(I-S.K.)

doi:10.1111/j.1582-4934.2007.00189.x

becomes more bulky, atherosclerotic plaques may develop into plaque that is vulnerable to rupture (vulnerable plaque) and its rupture causes the formation of thrombosis [1].

Conventional atherosclerosis imaging with x-ray angiography reveals only the severity of luminal narrowing of vessel and does not take into account the plaque biology, including vulnerable plaque [3]. Although some catheter-based techniques, such as intravascular ultrasound, can provide information on the composition of individual plaques, their invasive nature limits their use [4]. Therefore, there still remains a great need for novel diagnostic tools to assess non-invasively molecular changes associated with atherosclerosis and to understand plaque nature for detecting whether the plaque is vulnerable to impending rupture or stable atherosclerotic lesion.

Phage-displayed peptide library has been used to find novel peptide ligands that target specific organs, tumours, and tumour blood vessels [5–7]. Such tissue-specificity is based on the molecular diversity of tissues and blood vessels. Angiogenic tumour blood vessels, for example, are morphologically tortuous and leaky and carry distinct molecular markers like $\alpha v\beta 3$ integrin on the endothelium [8, 9], leading to the identification of the tumour vasculature-homing Arg-Gly-Asp (RGD) peptide [10]. Similarly, atherosclerotic blood vessels have characteristic molecular changes, including increased expression of vascular cell adhesion molecule-1 (VCAM-1) and P-selectin on endothelial surface and the formation of new blood vessels (vasa vasorum) in the arterial wall [1].

Identification of targeting ligands that home specifically to atherosclerotic plaques may provide numerous potential applications including selective delivery of therapeutic agents and imaging probes to plaque tissues. Such tissue-specific homing ligands may also lead to the identification of novel receptors and new drug targets at the lesion. Peptides have several advantages over antibodies as a targeting moiety, including better organ penetration and less chance of unintended immune reaction [11]. Here we used phage display technology and identified peptides that selectively recognize and home to atherosclerotic plaques *in vivo*.

Materials and methods

Animals

Male low-density lipoprotein receptor-deficient (*Ldlr*$^{-/-}$) mice on a C57BL/6 background (B6.129-*Ldlr*^{tm1Her}) were fed with a high-cholesterol atherogenic diet containing 15% fat, 1.25% cholesterol, and 0.5% Na-cholate (Oriental Yeast Co. Ltd.) for 8 weeks from 6 week old. As control, C57BL/6j male mice were maintained on regular chow diet for the same days. Mice were housed at 22 ± 2°C, 55 ± 5% relative humidity, with a light/dark cycle of 12 hr. Food (Purina Mills) and water were given *ad labium*. Body weights of mice at the time of experiments were 25–30 gm. All experiments were approved by the Kyungpook National University Animal Experiment Ethics Committee.

Ex vivo screening of a phage library

Primary human atherosclerotic tissues were obtained by endarterectomy of three patients with coronary atheroma (50 ± 12 year-old) and three patients with femoral atheroma (63 ± 11 year-old). Cell suspensions were prepared by homogenizing the tissues using Medimachine™ (DAKO). All primary human tissues were obtained according to the guidelines of Kyungpook National University.

We used a phage library displaying $C^{X7}C$ (C, cysteine; X, any amino acid residue) random peptides, which was built in the T7 415-1b vector (Novagen) between EcoRI and HindIII sites. X residues are encoded by NNK. The library had a diversity of approximately 5×10^8 plaque-forming unit (pfu). Screening of a phage library was performed as previously described [6]. The cell suspension was incubated with phage library (1×10^9 pfu) at 4°C for 2 hr. Unbound phages were removed by serially washing with Dulbecco's modified Eagle's medium (DMEM)/1% bovine serum albumin (BSA). The cell-bound phages were rescued by treating with 1% NP-40 on ice for 5 min. and adding BL21 host bacteria to the lysates. The phage output in pfu was determined by counting the number of plaques. The eluted phages were propagated in bacterial cells and used for the next round of selection. After three to four rounds of selection, individual clones were randomly picked from the clones of final two rounds of screening. The DNA inserts of selected phage clones were sequenced by automatic sequencer (Koma Biotech Co., Daegeon, Korea). The peptide sequences were analysed with the Clustal W program to align amino acid sequences and with the NCBI BLAST search to identify proteins with homologous motifs.

In vivo homing assays

A selected phage clone (1×10^{11} pfu in 100 µl solution) was injected into the tail vein of mice anesthetized by the inhalation of enflurane. After 15 min. of circulation, mice were perfused with phosphate-buffered saline (PBS) through the heart. Aortas were isolated and homogenized. The bounded phages were recovered and the phage titre was measured.

A fluorescein-conjugated synthetic peptide (100 µl of 1 mmol/l solution) was injected into the left ventricle of anaesthetized mice. After 15 min. of circulation, mice were perfused with PBS and then with 4% paraformaldehyde (PFA). Aorta and other organs were isolated and prepared for frozen section. Serially sectioned tissues in 5 µm thickness were immunostained with rabbit anti-mouse von Willebrand Factor (vWF) (Abcam Ltd., 1:5000), rat anti-mouse Mac3 (BD Pharmingen, 1:50), and Rat anti-mouse interleukin-4 receptor (IL-4R) (BD Pharmingen, 1:400) antibodies for 1 hr at room temperature (RT). Alexa568-conjugated goat anti-rabbit or anti-rat IgG (Molecular Probe) was used as a secondary antibody at 1:200 dilutions and incubated for 30 min. at RT. After mounting with the media containing 4-6 diaridino-2-phenylindole (DAPI) (Vector Laboratories) for nuclear counterstaining, tissue slides were visualized under a fluorescent microscope (Zeiss).

Fluorescein-conjugated peptides were synthesized by standard Fmoc method using a peptide synthesizer (Anygen Co., Kwangju, Korea). Fuorescein was conjugated to the N-terminus of peptides using aminocaproic acid as a linker. Synthetic peptides were purified by high-performance liquid chromatography (HPLC) and analysed by mass spectroscopy. The purities of separated peptides were higher than 85%. For making working solutions, peptides were dissolved with dimethylsulfoxide at the concentration of 100 mmol/l, diluted to the concentration of 1 mmol/l, and then stored in aliquots at −20°C.

Peptide overlay onto primary tissues

Primary tissues used for peptide overlay were femoral or coronary atherosclerotic tissues from three patients (62 ± 6 year-old) and a normal peroneal artery tissue from a patient who received by-pass surgery (39 year-old). Tissues were immersion fixed in 4% PFA for 2 hrs, incubated overnight in 25% sucrose/PBS for cryoprotection, embedded in optimal cutting temperature (OCT) medium, and then frozen. Sections in 5 μm thickness were prepared on a cryostat. The frozen sections were blocked with PBS/1%BSA at RT for 30 min., incubated with the 10 mol/l solution of a fluorescein-labelled peptide in PBS at RT for 1 hr, and then washed with PBS. Serial sections were immunostained with mouse anti-human CD31 (Chemicon, 1:50), mouse anti-human CD68 (Abcam Ltd., 1:100), mouse anti-human α-smooth muscle actin (α-SMA) (Sigma-Aldrich Inc., 1:2000), and mouse anti-human IL-4R (R&D systems, 1:500) antibodies for 1 hr at RT. Goat Alexa594-conjugated anti-mouse IgG (1:400) was used as a secondary antibody. H&E staining for histological examination and Oil Red O staining for lipid were performed by standard methods. After mounting with the media containing DAPI for nuclear counterstaining, tissue slides were visualized under a fluorescent microscope.

Overexpression and knockdown assays

Human IL-4R expression vector (OriGene technologies, Inc., Rockville, MD, USA) or control pCMV vector was transfected into semi-confluent Chinese hamster ovary (CHO)-K1 cells using Lipofectamine™ transfection agent (GIBCO-BRL). CHO-K1 cells (ATCC CCL-61) were maintained in α-minimum essential medium (MEM) containing 10% foetal bovine serum (FBS) at 37°C. For transfection, cells (1×10^4 cells per well of 4-well chamber slide) were incubated with the mixture of DNA (4 μg per well) and the transfection agent for 6 hrs in Opti-MEM™ (GIBCO-BRL). The medium was then changed to α-MEM with 10% FBS and incubated for additional 48 hrs.

For knockdown assays, pre-designed siRNA against human IL-4R (Ambion) was transfected into HT-1376 cells using lipid-based siPORT™ NeoFX™ transfection agent (Ambion). HT-1376 human bladder tumour cells (ATCC CRL-1472) were maintained in MEM supplemented with 10% FBS, non-essential amino acids and penicillin/streptomycin at 37°C. For transfection, cells (2×10^4 cells per well of 4-well chamber slide) were incubated with the mixture of siRNA at the 10 nmol/l concentration (67 ng) and the transfection agent for 48 hrs in Opti-MEM. The medium was then changed to MEM with 10% FBS and incubated for additional 24 hrs. A control siRNA (Ambion), not known to have any homology to any known mammalian gene, was used at the same concentration as a negative control.

After transfection, cells were fixed with cold methanol-acetone (1:1) for 10 min. and stained with mouse anti-human IL-4R antibody (1:400). Goat Alexa594-conjugated antimouse IgG (1:400) was used as a secondary antibody. After IL-4R staining, cells were incubated with the 10 μmol/l solution of the fluorescent peptide for 1 hr at RT. After mounting with the medium containing DAPI, tissue slides were visualized under a fluorescent microscope.

For flow cytometry, transfected cells were harvested with trypsin, blocked with 1% BSA at 37°C for 30 min., and then incubated with the 10 μmol/l solution of the fluorescent peptide for 1 hr at 4°C. After incubation, cells were washed with PBS and the percent number of fluorescent (peptide-bound) cells was analysed using a flow cytometry (Becton Dickinson).

Radioisotope labelling of peptides and autoradiography

The CRKRLDRNC peptide was conjugated with diethylenetriaminepentaacetic acid (DTPA) at the N-terminus and cyclized through disulfide bond between N- and C-terminus cysteines. [^{111}In]$InCl_3$ ($T_{1/2}$ = 67 h) was purchased from Perkin Elmer Life and Analytical Sciences. The DTPA-CRKRLDRNC peptide (5 μg in 10 μl PBS) was incubated with a solution of [^{111}In]$InCl_3$ (680 μCi in 100 μl of 0.1 M ammonium acetate, pH 5.5) for 1 hr at RT.

The CLEVSRKNC peptide was added with a tyrosine residue at the N-terminus during synthesis and cyclized through disulfide bond between two cysteine residues. [^{123}I]NaI ($T_{1/2}$ = 13 h) was purchased from Korea Institute of Radiology and Science. Iodobead (Pierce) was incubated with a solution of [^{123}I]NaI (3 mCi in 100 μl PBS) and then with the Y-CLEVSRKNC peptide (14 μg in 20 μl water) for 15 min. at RT. The labelled peptides were purified by RP-HPLC in gradient solvent system. The radiochemical yield of final solution was measured to be over 95%.

For autoradiography, the labelled peptide was injected into mice through the tail vein. After 15 min. of circulation, mice were perfused with PBS through the heart. Aortas were isolated, fixed for 1 hr in 4% PFA, and placed in parallel position in an X-ray cassette. A transparency film was stretched over the aortas. A photographic film (agfa) was pressed against the transparency film and then exposed.

Statistical analysis

ANOVA test was used to analyse mean values, and a *P*-value of <0.05 was considered statistically significant.

Results

Screening of a phage-displayed peptide library

A T7 phage library displaying random peptides was screened to enrich phages that selectively bind to atherosclerotic plaques. We performed *ex vivo* screening with cell suspension from human atherosclerotic plaque tissues obtained by coronary atherectomy or femoral endarterectomy. The cell-bound phages were recovered and amplified for the next round of screening. After three rounds of screening with coronary atheroma and four rounds with femoral atheroma, the phage titres were enriched approximately by 500-fold and 120-fold, respectively (data not shown).

Fifty-four phage clones from coronary and femoral atheroma tissues were randomly picked. The peptide-coding DNA inserts of the phage clones were amplified by PCR and sequenced. Alignment analysis of the peptide sequences using Clustal W program revealed frequently occurring sequences such as CRKRLDRNC or shared motifs with the length of three to four amino acids, such as GKRD (Table 1). The CRKRLDRNC sequence was the most frequently occurring one among selected peptide

Table 1 Selected peptide sequences and example of human proteins containing the homologous motif

Peptide sequence	Frequency	Homologous motif	Example of homologous proteins	Accession number
Coronary				
CRKRLDRNC	8/27(30%)	^{84}KRLDRN^{89}	IL-4	P05112
CMNPKKQRC	4/27(15%)	^{762}MNPK^{765}	Integrin β2 precursor	P05107
CRSTKSSAC	2/27(7.5%)	^{68}TKSSA^{72}	Thrombospondin-4 precursor	P35443
Femoral				
CPSNGKRDC CRQGGKRDC	2/27(7.5%) 1/27(3.8%)	^{177}NGKRD^{181}	MMP-16	P51512
CRTTRSKTC CRTTQSNTC	1/27(3.8%) 1/27(3.8%)	^{266}RTTSTKT^{272}	Scavenger receptor class A member 3	P35443
CFSEVD CMHSEVD CLIGEVD	2/27(7.5%) 1/27(3.8%) 1/27(3.8%)	^{367}FSEVD^{371}	Toll-like receptor 4 precursor	O00206

Peptides were analysed using the NCBI BLAST search against the SWISSPROT database, using the option for short nearly exact matches, to identify proteins with homologous motifs. Underlined letters represent shared motifs among the selected peptides. Frequency = (number of the peptide with the same sequence/total number of peptides). Numbers in parenthesis represent frequency in percentage.

sequences and thus prioritized for further study. Table 1 also lists selected example of human proteins shown by database search to contain motifs homologous to the peptides. The phage-displayed peptides may mimic one or more of these proteins in atherosclerotic plaque binding.

In vivo homing and localization of the CRKRLDRNC peptide at atherosclerotic plaques

We validated *in vivo* homing of the individual phage displaying the CRKRLDRNC peptide to atherosclerotic plaques. The CRKRLDRNC-phage (10^{11} pfu) was administrated into the tail vein of *Ldlr*$^{-/-}$ mice or age-matched C57BL/6 mice as control and allowed to circulate for 15 min. Aortas including aortic arch were isolated and bound phages were recovered. The CRKRLDRNC-phage homed to atherosclerotic aortic tissues of *Ldlr*$^{-/-}$ mice at approximately 8-fold higher level than to normal aortic tissues of wild-type mice (Fig. 1, *Ldlr*$^{-/-}$ mice versus control, $P<0.05$, n = 3). In addition, the CRKRLDRNC-phage bound to atherosclerotic tissues at higher level than did nonrecombinant (or insertless) control phage (Fig. 1, CRKRLDRNC vs. insertless, $P<0.05$, n = 3).

Next, we examined whether the selective homing of the CRKRLDRNC-phage to atherosclerotic plaque tissues was mediated by the peptide displayed on the phage. To address this question, a fluorescein-conjugated synthetic CRKRLDRNC peptide was

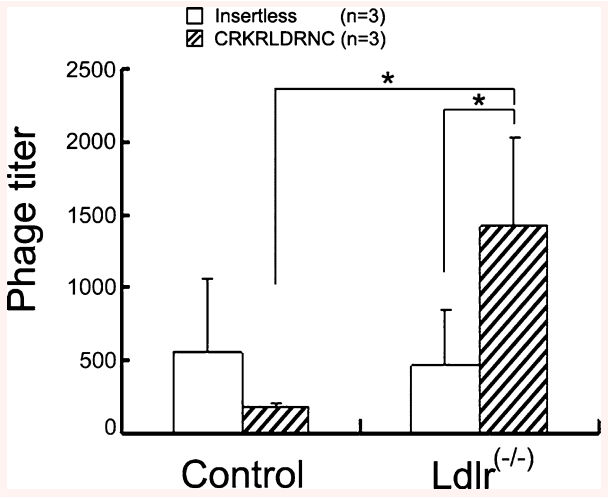

Fig. 1 *In vivo* homing of the CRKRLDRNC-phage to atherosclerotic plaque tissues. The CRKRLDRNC-phage or insertless control phage (10^{11} pfu) was intravenously injected into the tail vein of *Ldlr*$^{-/-}$ or C57BL/6 control mice and circulated for 15 min. Aortic tissues were isolated and bound phages were recovered. Data represent mean ± SD of measurements of phage titer (pfu per 10 mg tissue). n, number of animals examined in each experiment. *, $P< 0.05$ by ANOVA test.

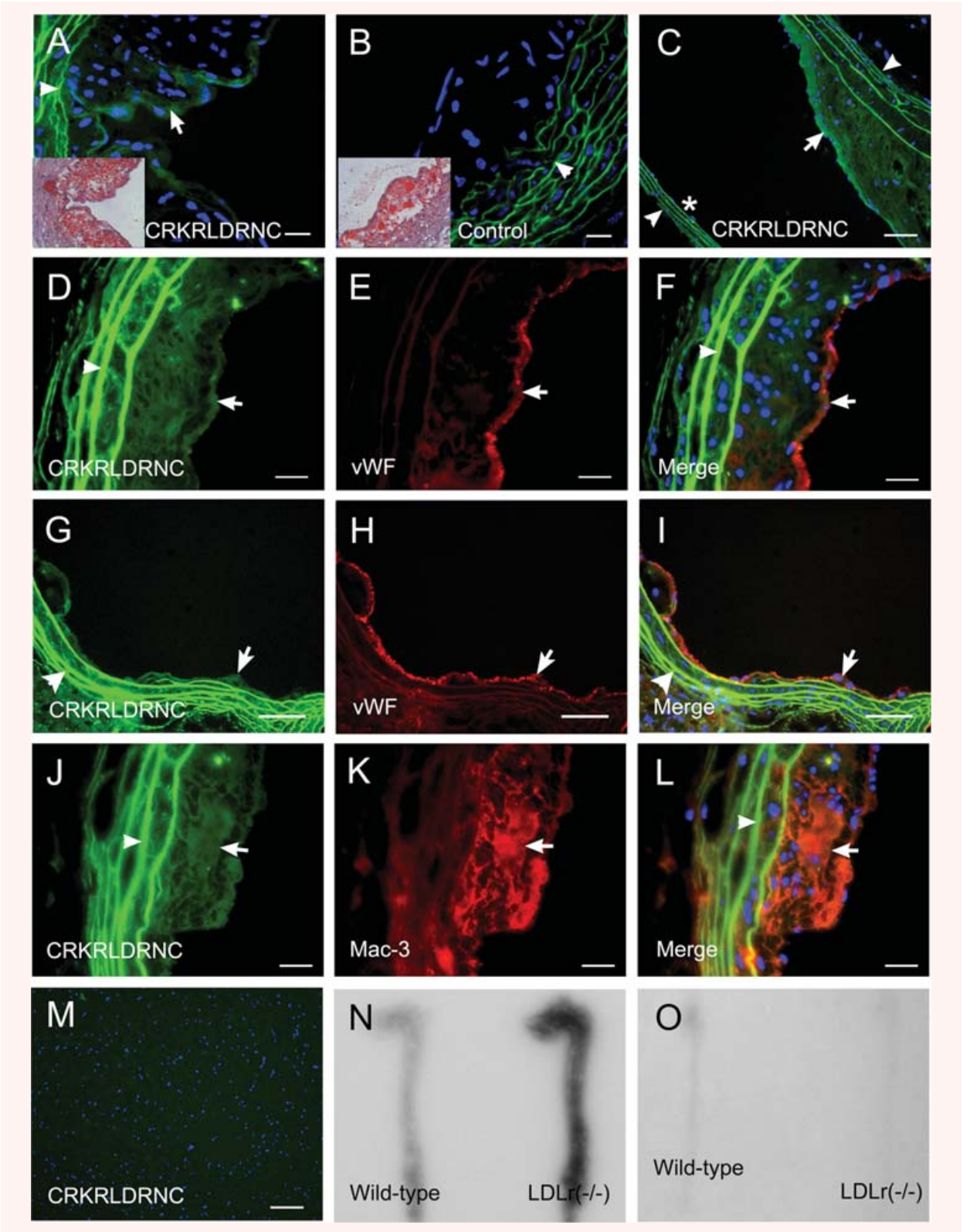

Fig. 2 *In vivo* homing of the CRKRLDRNC peptide to atherosclerotic plaques in *Ldlr*$^{-/-}$ mice. A fluorescein-labelled peptide was injected into the left ventricle of *Ldlr*$^{-/-}$ mice and circulated for 15 min. (**A**–**C**) *In vivo* homing of the fluorescent CRKRLDRNC peptide (**A** and **C**) or NSSSVDK control peptide (**B**) to atherosclerotic plaques of *Ldlr*$^{-/-}$ mice. Insets show Oil red-O staining of lipid deposition in the plaques. Note that the CRKRLDRNC peptide bound to the endothelium overlying lesions (arrows in **A** and **C**), but not to the endothelium not directly overlying lesions (asterisk in **C**). (**D**–**L**) The CRKRLDRNC peptide binding (**D**, **G** and **J**), co-staining for vWF (**E** and **H**) or Mac-3 (**K**), and the merges (**F**, **I** and **L**). Note the co-localization of the peptide with endothelial cells (arrows in **D**–**I**) and macrophages (arrows in **J**–**L**). (**M**) The CRKRLDRNC peptide in brain. Arrowheads in (**A**–**L**) show autofluorescence resulted from elastic tissue in the vessel wall. DAPI staining for nucleus was shown in blue. Scale bars represent 20 μm (**A**–**L**) and 100 μm (**M**). (**N** and **O**) ^{111}In-labeled CRKRLDRNC peptide at 160 μCi (**M**) or ^{123}I-labelled CLEVSRKNC control peptide at 104 μCi (**O**) was injected into the tail vein of *Ldlr*$^{-/-}$ or wild-type mice and circulated for 15 min. Representative autoradiographs were shown for the experiments.

injected into the left ventricle of *Ldlr*$^{-/-}$ or control mice and circulated for 15 min. In previous studies, peptides that home to tumour blood vessels were allowed to circulate for a short period of time (*e.g.* 5–10 min.) [5–7]. We reasoned that homing of a peptide to atherosclerotic lesions could also be achieved at a similar period of time. Oil red-O staining of frozen sections demonstrated lipid deposition at atherosclerotic plaques in the aortas of *Ldlr*$^{-/-}$ mice (Fig. 2A and B, insets). The CRKRLDRNC peptide homed to atherosclerotic plaques of three *Ldlr*$^{-/-}$ mice (Fig. 2A), while the NSSSVDK control peptide, the sequence that is displayed by the nonrecombinant T7 phage, did not (Fig. 2B). The homing peptide bound to the endothelium overlying a lesion, but not to the endothelium not directly overlying the lesion (non-atherosclerotic area) of the same mouse (Fig. 2C). The CRKRLDRNC peptide did not home to other organs such as brain (Fig. 2M) as well as liver and lung (not shown). Similar results were obtained when the peptide was circulated for 2 hr (data not shown).

To see the type of cellular components to which the homing peptide bound *in vivo*, we analysed the localization of the CRKRLDRNC peptide at the atherosclerotic plaques of *Ldlr*$^{-/-}$ mice. Immunostaining using antibodies against the cell-type specific markers showed that the fluorescent CRKRLDRNC peptide co-localized with endothelial cells (vWF) along the surface of atherosclerotic plaques (Fig. 2D–F) and also macrophages (Mac3) inside the plaques (Fig. 2J–L). Interestingly, the homing peptide also could bind to early atherosclerotic lesions of relatively small size (Fig. 2G–I).

We further examined *in vivo* homing of the peptide by labelling it with a radioisotope. The ^{111}In-labeled CRKRLDRNC peptide or ^{123}I–labelled CLEVSRKNC peptide was injected into the tail vein of *Ldlr*$^{-/-}$ or control mice and circulated for 15 min. The CLEVSRKNC peptide, a peptide containing CX7C amino acids of unrelated sequence, was used as control. The aortas were isolated and subjected to autoradiography. As expected, ^{111}In-CRKRLDRNC uptake was clearly observed at aortas of three *Ldlr*$^{-/-}$ mice, while little uptake was observed at aortas of three wild-type mice (Fig. 2N). In contrast, ^{123}I–CLEVSRKNC uptake was negligible at aortas of both *Ldlr*$^{-/-}$ and control mice (Fig. 2O). The uptake signal in Fig. 2N was observed diffusely, rather than focally, along the aortas, which reflects the radiating property of radioisotope signals.

The CRKRLDRNC peptide overlay onto human atherosclerotic plaques

To examine whether the CRKRLDRNC peptide selectively binds to human atherosclerotic plaques, we performed peptide overlay onto frozen sections of primary tissues. Oil red-O staining demonstrated characteristic lipid deposition at atherosclerotic plaques (Fig. 3A). The fluorescein-labelled CRKRLDRNC peptide bound to the sections of eight atherosclerotic tissues from human arteries (Fig. 3B), while little binding of the NSSSVDK control peptide was observed (Fig. 3C). In similar to the localization of the peptide at mouse tissues *in vivo*, the CRKRLDRNC peptide co-localized with endothelial cells (CD31) (Fig. 3 D-F), macrophages (CD68) (Fig. 3G–I), and vascular smooth muscle cells (alpha-SMA) (Fig. 3J–L) on the sections of two atherosclerotic plaques. These results suggest that a putative binding receptor for the homing peptide exits on those multiple cellular components of atherosclerotic plaques.

IL-4R as a candidate target receptor for the CRKRLDRNC homing peptide

Homology search by a protein database revealed that the RKRLDRN sequence matched, in six out of seven positions, the ^{84}KRLDRN^{89} motif of an inflammatory cytokine IL-4 (Table 1). The main binding determinants of human and mouse IL-4 (Fig. 4A, underlined) have been previously described [12, 13]. To our interest, the KRLDRN motif is the core of the binding site of human IL-4 for IL-4R, the corresponding receptor. Moreover, the amino acid sequences of the binding site, as shown in Figure 4A, are conserved among species, such as human, cat and deer [13]. These findings suggest that the CRKRLDRNC peptide may mimic IL-4 in atherosclerotic plaque binding. To investigate the hypothesis that the CRKRLDRNC peptide was homing to atherosclerotic plaques by virtue of this homology, we first analysed the localization of IL-4R at atherosclerotic plaques. IL-4R was abundantly present at atherosclerotic plaques in *Ldlr*$^{-/-}$ mice (Fig. 4C). The fluorescent CRKRLDRNC peptide, when injected into three *Ldlr*$^{-/-}$ mice, co-localized with IL-4R at atherosclerotic plaques (Fig. 4B–D).

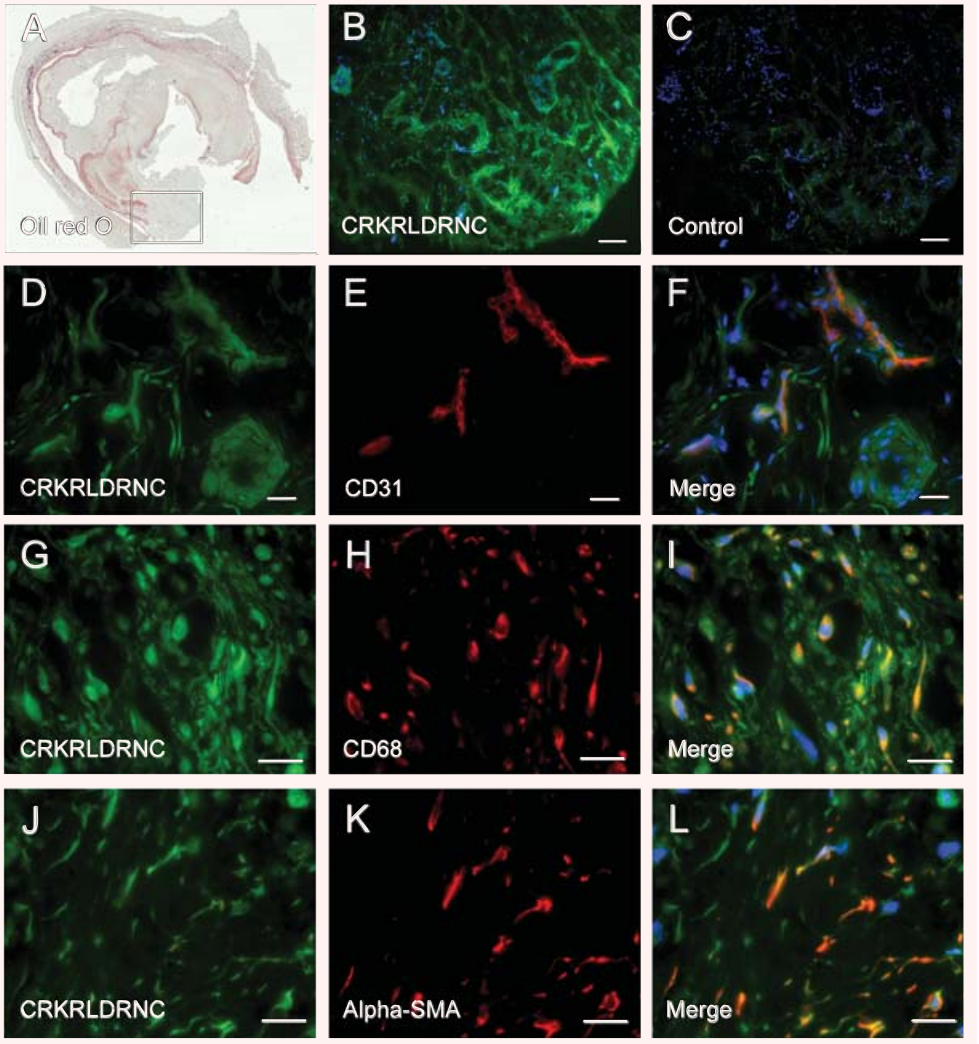

Fig. 3 The CRKRLDRNC peptide overlay onto human atherosclerotic plaques. (A) Oil red-O staining of a frozen section of atherosclerotic plaque from a human femoral artery. The box in (A) marks an area of the artery that was examined microscopically in (B–L). (B and C) Peptide overlay was performed with fluorescein-labelled CRKRLDRNC peptide (B) or NSSSVDK control peptide (C). (D–L) The CRKRLDRNC peptide overlay (D, G and J), co-staining for CD31 (E), CD68 (H) and α-SMA (K), and the merges (F, I and L). Note that the CRKRLDRNC peptide co-localized with endothelial cells, macrophages, and vascular smooth muscle cells at human atherosclerotic plaques. DAPI staining for nucleus was shown in blue. Scale bars represent 100 μm (B and C) and 20 μm (D–L).

Co-localization of the peptide and IL-4R was also observed by peptide overlay on two human atherosclerotic plaques (Fig. 4E–G). IL-4R was abundant in human atherosclerotic tissues (Fig. 4F), while being at negligible levels in a normal arterial tissue (Fig. 4H–I). These findings suggest that IL-4R is a candidate receptor for the peptide homing to atherosclerotic plaques.

To further investigate the hypothesis that IL-4R is the corresponding receptor for the homing of the CRKRLDRNC peptide, we transiently transfected the human IL-4R expression vector into CHO-K1 cells. Immunostaining showed that IL-4R is present at negligible levels in the parental (data not shown) or mock-transfected CHO-K1 cells (Fig. 5A), while it is expressed at high levels in the IL-4R-transfected cells (Fig. 5D). The fluorescent CRKDLDRNC peptide did not bind to the mock-transfected CHO-K1 cells (Fig. 5B). In contrast, the CRKDLDRNC peptide strongly bound to the CHO-K1 cells over-expressing IL-4R on the surface (Fig. 5D–F), while the binding of the NSSSVDK control peptide to the cells was minimal (Fig. 5C).

Next, we carried out the knockdown of IL-4R using siRNA in IL-4R-expressing cells. We examined several cell lines for endogenous expression of IL-4R on the cell surface. Immunostaining of IL-4R showed the expression of IL-4R at high levels in HT-1376 human bladder tumour cells (Fig. 5G) and HUVEC human endothelial cells (data not shown). The fluorescent CRKRLDRNC peptide strongly bound to HT-1376 cells (Fig. 5G–I), whereas the NSSSVDK control peptide did not (Fig. 5O). The binding of the fluorescent CRKRLDRNC peptide to the cells was completely blocked by the unlabeled (not fluorescent) CRKRLDRNC peptide given at 100-fold molar excess (data not shown). Transfection of the siRNA against human IL-4R almost suppressed its expression in HT-1376 cells (Fig. 5J). Accordingly, the binding of the CRKRLDRNC peptide to the cells was decreased to minimal levels (Fig. 5K–L).

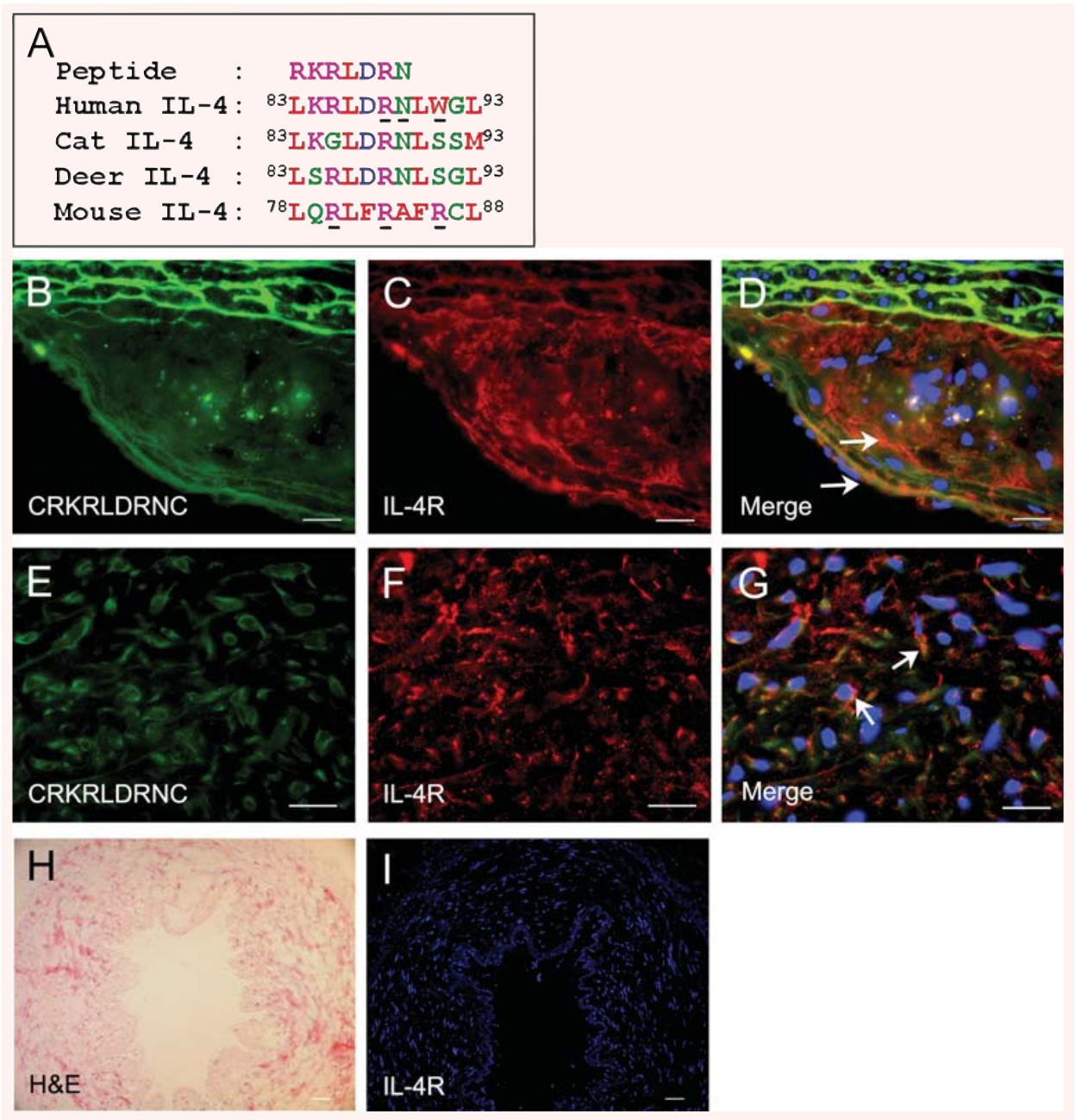

Fig. 4 Co-localization of the CRKRLDRNC peptide with IL-4R at mouse and human atherosclerotic plaques. (**A**) Amino acid sequences of human, cat, deer, and mouse IL-4 homologous to the CRKRLDRNC peptide. Amino acid colours are coded according to their biochemical properties: purple, basic; blue, acidic; green, hydrophilic; red, hydrophobic. The main binding determinants of human and mouse IL-4 for IL-4R were previously reported and underlined. (**B**–**D**) *In vivo* localization at atherosclerotic plaques of the fluorescein-labelled CRKRLDRNC peptide in *Ldlr*$^{-/-}$ mice (**B**), IL-4R staining (**C**) and the merge (**D**). (**E**–**G**) The CRKRLDRNC peptide overlay onto human atherosclerotic plaques (**E**), IL-4R staining (**F**) and the merge (**G**). Note that the CRKRLDRNC peptide co-localized with IL-4R, which was present at mouse and human atherosclerotic plaques (arrows in **D** and **G**). (**H**) H&E and (**I**) IL-4R staining of a human normal arterial tissue. DAPI staining for nucleus was shown in blue. Scale bars represent 20 μm (**B**–**G**) and 100 μm (**I**).

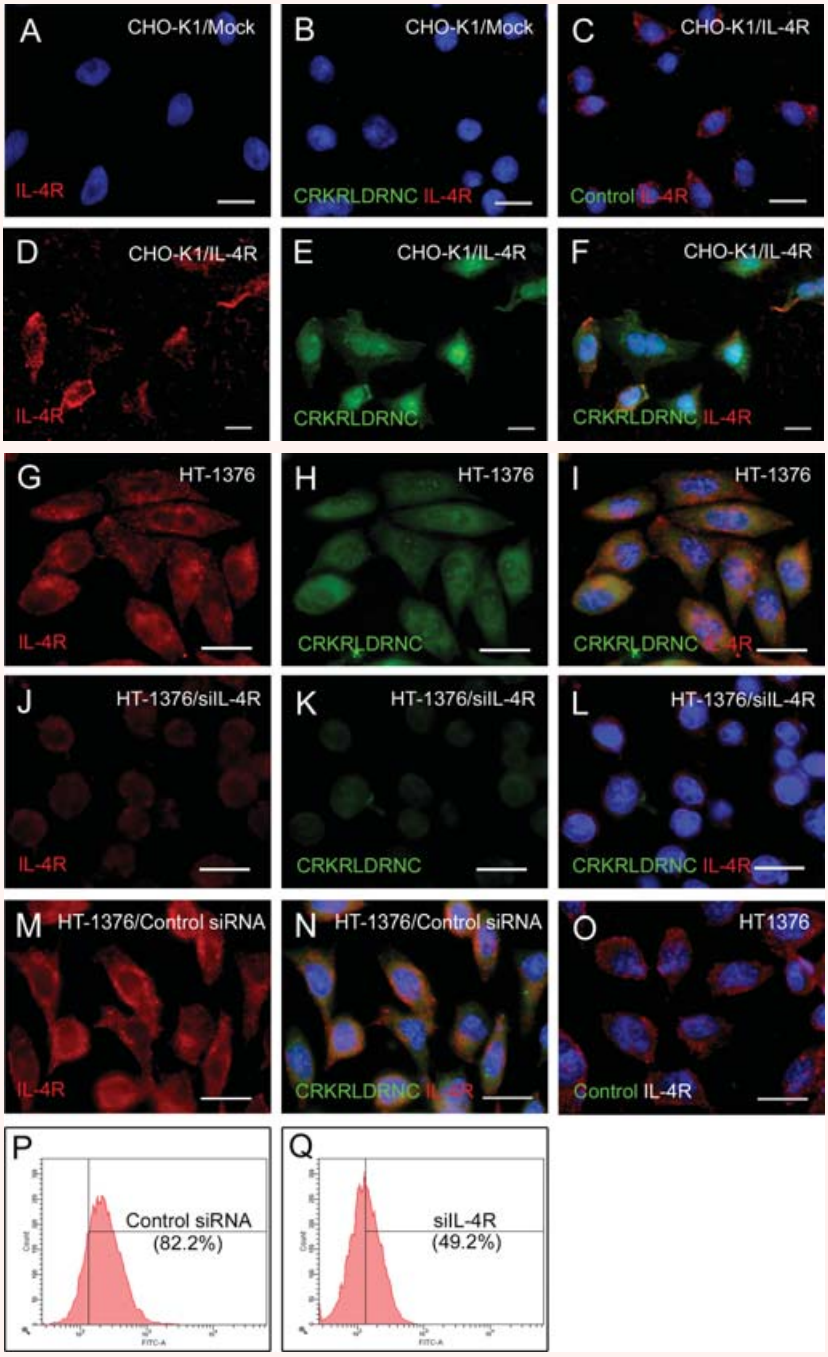

Fig. 5 The binding of the CRKRLDRNC peptide to IL-4R-expressing cells. (**A–O**) Cells were immunostained for IL-4R and then incubated with the indicated fluorescein-labelled peptide. IL-4R staining (**A**) and the merge with the CRKRLDRNC peptide binding (**B**) in mock-transfected CHO-K1 cells. The merge of IL-4R staining and the control peptide binding in IL-4R-transfected CHO-K1 cells (**C**) and HT-1376 cells (**O**). IL-4R staining, the CRKRLDRNC peptide binding, and the merges in IL-4R-transfected CHO-K1 cells (**D–F**), HT-1376 cells (**G–I**), and IL-4R siRNA-transfected HT-1376 cells (**J–L**). IL-4R staining (**M**) and the merge with the CRKRLDRNC peptide binding (**N**) in control siRNA-transfected HT-1376 cells. Note that the CRKRLDRNC peptide bound to cells expressing IL-4R on the cell surface and the binding was inhibited by the knockdown of the IL-4R expression. DAPI staining for nucleus was shown in blue. Scale bars represent 20 μm. (**P** and **Q**) HT-1376 cells transfected with control siRNA (**P**) or IL-4R siRNA (**Q**) were incubated with the CRKRLDRNC peptide and the percent number of peptide-bound cells (in parenthesis) was analysed by flow cytometry.

Control siRNA did not affect the expression of IL-4R in HT-1376 cells (Fig. 5M) and also the binding of the CRKRLDRNC peptide to the cells (Fig. 5N). In addition, the percent number of peptide-bound cells analysed by flow cytometry was decreased from 82.2% to 49.2% by the knockdown of IL-4R (Fig. 5P–Q). Together, these results demonstrate that IL-4R is the corresponding receptor for the binding of the CRKRLDRNC homing peptide.

Discussion

In this study, we demonstrated that the CRKRLDRNC peptide exhibited a selective homing to atherosclerotic plaques and that IL-4R is the corresponding receptor for the peptide binding. Using a phage-displayed random peptide library, we selected phages that bind to human primary atherosclerotic plaque tissues obtained from coronary or femoral arteries. Some of the peptide sequences frequently occurred or revealed shared motifs. Of these we validated the CRKRLDRNC peptide, the most frequently occurring sequence, as a promising atherosclerotic plaque-specific peptide. The fluorescein- or radioisotope-labelled CRKRLDRNC peptide homed to atherosclerotic plaques of *Ldlr*$^{-/-}$ mice. After being circulated through the blood, it homed to the atherosclerotic aorta, whereas homing to other organs such as brain and liver was minimal. Interestingly, it could recognize both early and late atherosclerotic lesions. Moreover, the peptide preferentially bound to human primary atherosclerotic tissue compared to normal tissue. These findings suggest that the binding receptor for the peptide is present at both early and late stage of atherosclerosis and conserved in both mouse and human species.

Protein database search for human proteins homologous to the CRKRLDRNC sequence revealed that this peptide has homology with the sequence between the residues 84 and 89 of human IL-4 (^{84}KRLDRN^{89}). Interestingly, it has been shown that five positively charged residues (K77, R81, K84, R85 and R88) and two neighbouring residues (N89 and W91) are important for binding of human IL-4 to IL-4R [12, 13]. The crystal structure of the complex reveals that residue R88 of the human IL-4 can form an ion pair with residue D72 of IL-4R [13]. In the murine IL-4, the main binding site is ^{79}QRLFRAFR^{86} and the underlined residues (R80, R83 and R86) play a crucial role for binding to the receptor [14]. Three arginine residues (underlined) of the CRKRLDRNC peptide may mimic those arginine residues of mouse IL-4 in binding to IL-4R. Similarity of a peptide to a receptor-binding ligand has been used for validation of the corresponding receptor as a target of the ligand-mimicking peptide (*e.g.* IL-11R and platelet-derived growth factor receptor β) [7, 15].

Several lines of evidence demonstrate that IL-4R is the corresponding receptor for the homing of the CRKRLDRNC peptide to atherosclerotic plaques. There are two types of IL-4R, a complex of IL-4R α chain with either IL-2R γc chain (type I IL-4R) or IL-13R α1 chain (type II IL-4R) [16]. Type I receptor is present in haematopoietic cells, while type II receptor is in haematopoietic cells of the myeloid lineage, such as macrophages and eosinophils, and in many other cell types, such as endothelial cells and fibroblasts [17, 18]. IL-4R also exits on T lymphocytes and vascular smooth muscle cells [19, 20]. First, we demonstrated that the CRKRLDRNC peptide injected into mice or subjected to peptide overlay onto human primary tissue co-localized with IL-4R at atherosclerotic plaques. We also demonstrated the up-regulation of IL-4R at both mouse and human atherosclerotic tissues, which was consistent with a previous study [21]. Second, the CRKRLDRNC peptide co-localized with endothelial cells, macrophages and smooth muscle cells, on which IL-4R is known to exist. Third, after the transient overexpression of IL-4R on CHO cells that do not have endogenous IL-4R, cells were able to bind with the peptide. The knockdown of IL-4R expression, on the other hand, on HT-1376 cells that have high levels of endogenous IL-4R deleted the binding of the peptide to the cells.

A growing body of evidence indicates that IL-4 is pro-atherogenic and contributes to the development of atherosclerosis. IL-4 is a pleiotropic immunomodulatory cytokine secreted by T-helper 2 (Th2) lymphocytes, eosinophils and mast cells [22]. First, IL-4 is detected at elevated levels in atherosclerotic lesions [23]. It induces inflammatory mediators, such as VCAM-1 and MCP-1 in vascular endothelial cells and matrix metalloproteinases (MMPs) in vascular smooth muscle cells [23–25]. Second, it induces apoptosis of endothelial cells through the caspase-3 pathway [26], which may cause the dysfunction of the vascular endothelium and the initiation of atherogenesis. Third, down-regulation of IL-4 secretion of Th2 cells inhibited Th2-mediated isotype switching and reduced atherosclerotic lesion formation in *Ldlr*$^{-/-}$ mice [27]. Most importantly, the knockout of IL-4 showed reduced size of atherosclerotic lesions in *Ldlr*$^{-/-}$ or apolipoprotein E-deficient (*ApoE*$^{-/-}$) mice [28, 29]. Interrogation of such a role for IL-4/IL-4R interaction during atherogenesis may be a novel therapeutic approach to atherosclerosis. The possibility that the CRKRLDRNC peptide may act as an antagonist (or agonist) for IL-4 action deserves future investigation.

Molecular imaging tools have been developed for the detection of early atherosclerotic lesion or vulnerable plaque based on the plaque biology. Current candidate targets include molecules, such as VCAM-1, P-selectin and ED-B fibronectin [30–32]. For example, a VCAM-1-binding peptide as the corresponding ligand was conjugated to magnetofluorescent nanoparticles and applied to the detection of atherosclerotic plaques in *ApoE*$^{-/-}$ mice [30, 33]. Detection of apoptosis using annexin V and proteolytic activities like MMPs and cathepsin B have been applied to the imaging of vulnerable plaques [34–36]. Activation of inflammatory process within plaques is also closely correlated with plaque rupture and clinical events. In a recent study, IL-2, a pro-inflammatory cytokine that binds to IL-2R on activated T lymphocytes, was labelled with a radioisotope and used for imaging of vulnerable plaques in human patients [37]. In this paper, we identified IL-4R and the CRKRLDRNC peptide as a novel target and the corresponding ligand for atherosclerosis imaging. We identified the CRKRLDRNC peptide by screening of phage library with human atherosclerotic tissues and demonstrated that it may be useful for imaging of atherosclerosis in human as well as mouse. This is contrast to previous studies [38, 39], in which screening of phage library and evaluation of binding specificity of peptides were performed only in mice. Moreover, the homing peptide could detect the early lesions of atherosclerosis in mice. It was previously described that IL-4 and IL-4R are expressed at coronary atherosclerotic plaques from patients with stable or unstable angina [21]. In these regards, IL-4 and IL-4R interaction might be implicated in the development of vulnerable plaques or in early stage of atherogenesis. It needs further investigation whether the CRKRLDRNC peptide is useful for the detection of early or vulnerable plaques.

It is noteworthy that IL-4R is also up-regulated in some tumours, such as ovarian cancer and lung cancer and has been already used as a target for tumour therapy [40, 41]. Taken together, the CRKRLDRNC peptide and IL-4R may be useful as a targeting ligand and the corresponding receptor for selective delivery of therapeutic drugs and imaging probes to atherosclerotic plaques as well as tumours.

Acknowledgements

This work was supported by the Ministry of Science and Technology (F104AA010003-06A0101-00310) (to B-H Lee), No. RTI04-01-01 from the Regional Technology Innovation Program of the Ministry of Commerce, Industry and Energy (MOCIE) in Korea (to I-S Kim), and Brain Korea 21 Project in 2006.

References

1. **Libby P.** Inflammation in atherosclerosis. *Nature.* 2002; 420: 868–74.
2. **Ross R.** Atherosclerosis–an inflammatory disease. *N Engl J Med.* 1999; 340: 115–26.
3. **Choudhury RP, Fuster V, Fayad ZA.** Molecular, cellular and functional imaging of atherothrombosis. *Nat Rev Drug Discov.* 2004; 3: 913–25.
4. **Davies JR, Rudd JH, Weissberg PL.** Molecular and metabolic imaging of atherosclerosis. *J Nucl Med.* 2004; 45: 1898–907.
5. **Pasqualini R, Ruoslahti E.** Organ targeting *in vivo* using phage display peptide libraries. *Nature.* 1996; 380: 364–6.
6. **Lee SM, Lee EJ, Hong HY, Kwon MK, Kwon TH, Choi JY, Park RW, Kwon TG, Yoo ES, Yoon GS, Kim IS, Ruoslahti E, Lee BH.** Targeting bladder tumor cells *in vivo* and in the urine with a peptide identified by phage display. *Mol Cancer Res.* 2007; 5: 11–9.
7. **Joyce JA, Laakkonen P, Bernasconi M, Bergers G, Ruoslahti E, Hanahan D.** Stage-specific vascular markers revealed by phage display in a mouse model of pancreatic islet tumorigenesis. *Cancer Cell.* 2003; 4: 393–403.
8. **McDonald DM, Choyke PL.** Imaging of angiogenesis: from microscope to clinic. *Nat Med.* 2003; 9: 713–25.
9. **Ruoslahti E.** Specialization of tumour vasculature. *Nat Rev Cancer.* 2002; 2: 83–90.
10. **Pasqualini R, Koivunen E, Ruoslahti E.** Alpha v integrins as receptors for tumor targeting by circulating ligands. *Nat Biotechnol.* 1997; 15: 542–6.
11. **Ladner RC, Sato AK, Gorzelany J, de Souza M.** Phage display-derived peptides as therapeutic alternatives to antibodies. *Drug Discov Today.* 2004; 9: 525–9.
12. **Wang Y, Shen BJ, Sebald W.** A mixed-charge pair in human interleukin 4 dominates high-affinity interaction with the receptor alpha chain. *Proc Natl Acad Sci USA.* 1997; 94: 1657–62.
13. **Mueller TD, Zhang JL, Sebald W, Duschl A.** Structure, binding, and antagonists in the IL-4/IL-13 receptor system. *Biochim Biophys Acta.* 2002; 1592: 237–50.
14. **Yao G, Chen W, Luo H, Jiang Q, Xia Z, Zang L, Zuo J, Wei X, Chen Z, Shen X, Dong C, Sun B.** Identification of core functional region of murine IL-4 using peptide phage display and molecular modeling. *Int Immunol.* 2006; 18: 19–29.
15. **Chen L, Zurita AJ, Ardelt PU, Giordano RJ, Arap W, Pasqualini R.** Design and validation of a bifunctional ligand display system for receptor targeting. *Chem Biol.* 2004; 11: 1081–91.
16. **Andrews AL, Holloway JW, Holgate ST, Davies DE.** IL-4 receptor alpha is an important modulator of IL-4 and IL-13 receptor binding: implications for the development of therapeutic targets. *J Immunol.* 2006; 176: 7456–61.
17. **Nelms K, Keegan AD, Zamorano J, Ryan JJ, Paul WE.** The IL-4 receptor: signaling mechanisms and biologic functions. *Annu Rev Immunol.* 1999; 17: 701–38.
18. **Murata T, Obiri NI, Puri RK.** Structure of and signal transduction through interleukin-4 and interleukin-13 receptors (review). *Int J Mol Med.* 1998; 1: 551–7.
19. **Schnyder B, Lugli SM, Schnyder-Candrian S, Eng VM, Moser R, Banchereau J, Ryffel B, Car BD.** Biochemical and morphological characterization of vascular and lymphocytic interleukin-4 receptors. *Am J Pathol.* 1996; 149: 1369–79.
20. **Hulshof S, Montagne L, De Groot CJ, Van Der Valk P.** Cellular localization and expression patterns of interleukin-10, interleukin-4, and their receptors in multiple sclerosis lesions. *Glia.* 2002; 38: 24–35.
21. **Randi AM, Biguzzi E, Falciani F, Merlini P, Blakemore S, Bramucci E, Lucreziotti S, Lennon M, Faioni EM, Ardissino D, Mannucci PM.** Identification of differentially expressed genes in coronary atherosclerotic plaques from patients with stable or unstable angina by cDNA array analysis. *J Thromb Haemost.* 2003; 1: 829–35.
22. **Paul WE.** Interleukin-4: a prototypic immunoregulatory lymphokine. *Blood.* 1991; 77: 1859–70.
23. **Sasaguri T, Arima N, Tanimoto A, Shimajiri S, Hamada T, Sasaguri Y.** A role for interleukin 4 in production of matrix metalloproteinase 1 by human aortic smooth muscle cells. *Atherosclerosis.* 1998; 138: 247–53.
24. **Lee YW, Kuhn H, Hennig B, Neish AS, Toborek M.** IL-4-induced oxidative stress upregulates VCAM-1 gene expression in human endothelial cells. *J Mol Cell Cardiol.* 2001; 33: 83–94.
25. **Lee YW, Hennig B, Toborek M.** Redox-regulated mechanisms of IL-4-induced MCP-1 expression in human vascular endothelial cells. *Am J Physiol Heart Circ Physiol.* 2003; 284: H185–92.
26. **Lee YW, Kuhn H, Hennig B, Toborek M.** IL-4 induces apoptosis of endothelial cells through the caspase-3-dependent pathway. *FEBS Lett.* 2000; 485: 122–6.
27. **van Wanrooij EJ, van Puijvelde GH, de Vos P, Yagita H, van Berkel TJ, Kuiper J.** Interruption of the Tnfrsf4/Tnfsf4 (OX40/OX40L) pathway attenuates atherogenesis in low-density lipoprotein receptor-deficient mice. *Arterioscler Thromb Vasc Biol.* 2007; 27: 204–10.
28. **Davenport P, Tipping PG.** The role of interleukin-4 and interleukin-12 in the progression of atherosclerosis in apolipoprotein E-deficient mice. *Am J Pathol.* 2003; 163: 1117–25.
29. **King VL, Szilvassy SJ, Daugherty A.** Interleukin-4 deficiency decreases atherosclerotic lesion formation in a site-specific manner in female LDL receptor-/- mice. *Arterioscler Thromb Vasc Biol.* 2002; 22: 456–61.
30. **Kelly KA, Allport JR, Tsourkas A, Shinde-Patil VR, Josephson L, Weissleder R.** Detection of vascular adhesion molecule-1 expression using a novel multimodal nanoparticle. *Circ Res.* 2005; 96: 327–36.
31. **Molenaar TJ, Twisk J, de Haas SA, Peterse N, Vogelaar BJ, van Leeuwen**

SH, Michon IN, van Berkel TJ, Kuiper J, Biessen EA. P-selectin as a candidate target in atherosclerosis. *Biochem Pharmacol.* 2003; 66: 859–66.

32. **Matter CM, Schuler PK, Alessi P, Meier P, Ricci R, Zhang D, Halin C, Castellani P, Zardi L, Hofer CK, Montani M, Neri D, Luscher TF.** Molecular imaging of atherosclerotic plaques using a human antibody against the extra-domain B of fibronectin. *Circ Res.* 2004; 95: 1225–33.
33. **Kelly KA, Nahrendorf M, Yu AM, Reynolds F, Weissleder R.** *in vivo* phage display selection yields atherosclerotic plaque targeted peptides for imaging. *Mol Imaging Biol.* 2006; 8: 201–7.
34. **Kolodgie FD, Petrov A, Virmani R, Narula N, Verjans JW, Weber DK, Hartung D, Steinmetz N, Vanderheyden JL, Vannan MA, Gold HK, Reutelingsperger CP, Hofstra L, Narula J.** Targeting of apoptotic macrophages and experimental atheroma with radiolabeled annexin V: a technique with potential for noninvasive imaging of vulnerable plaque. *Circulation.* 2003; 108: 3134–9.
35. **Deguchi JO, Aikawa M, Tung CH, Aikawa E, Kim DE, Ntziachristos V, Weissleder R, Libby P.** Inflammation in atherosclerosis: visualizing matrix metalloproteinase action in macrophages *in vivo.* Circulation. 2006; 114: 55–62.
36. **Chen J, Tung CH, Mahmood U, Ntziachristos V, Gyurko R, Fishman MC, Huang PL, Weissleder R.** *in vivo* imaging of proteolytic activity in atherosclerosis. *Circulation.* 2002; 105: 2766–71.
37. **Annovazzi A, Bonanno E, Arca M, D'Alessandria C, Marcoccia A, Spagnoli LG, Violi F, Scopinaro F, De Toma G, Signore A.** 99mTc-interleukin-2 scintigraphy for the *in vivo* imaging of vulnerable atherosclerotic plaques. *Eur J Nucl Med Mol Imaging.* 2006; 33: 117–26.
38. **Houston P, Goodman J, Lewis A, Campbell CJ, Braddock M.** Homing markers for atherosclerosis: applications for drug delivery, gene delivery and vascular imaging. *FEBS Lett.* 2001; 492: 73–7.
39. **Liu C, Bhattacharjee G, Boisvert W, Dilley R, Edgington T.** *In vivo* interrogation of the molecular display of atherosclerotic lesion surfaces. *Am J Pathol.* 2003; 163: 1859–71.
40. **Kioi M, Takahashi S, Kawakami M, Kawakami K, Kreitman RJ, Puri RK.** Expression and targeting of interleukin-4 receptor for primary and advanced ovarian cancer therapy. *Cancer Res.* 2005; 65: 8388–96.
41. **Garland L, Gitlitz B, Ebbinghaus S, Pan H, de Haan H, Puri RK, Von Hoff D, Figlin R.** Phase I trial of intravenous IL-4 pseudomonas exotoxin protein (NBI-3001) in patients with advanced solid tumors that express the IL-4 receptor. *J Immunother.* 2005; 28: 376–81.